Langmuir

Article

pubs.acs.org/Langmuir

# Capillary Osmosis in a Charged Nanopore Connecting Two Large Reservoirs

Kuan-Liang Liu,[†] Jyh-Ping Hsu,*[,†] and Shiojenn Tseng*[,‡]

[†]Department of Chemical Engineering, National Taiwan University, Taipei, Taiwan 10617,

[‡]Department of Mathematics, Tamkang University, Tamsui, Taipei, 25137, Taiwan,

Supporting Information

**ABSTRACT:** Experimental evidence revealed that the performance of nanopore-based biosensing devices can be improved by applying a salt concentration gradient. To provide a theoretical explanation for this observation and explore the mechanisms involved, we model the capillary osmosis (or diffusioosmosis) in a charged solid-state nanopore connecting two large reservoirs. The effects of nanopore geometry and the reservoir salt concentrations are examined. We show that the capillary osmotic flow is from the high salt concentration reservoir to the low salt concentration one, and its magnitude has a maximum as the reservoir salt concentrations vary. In general, the shorter the nanopore and/or the smaller its radius, the faster the osmotic flow. This flow enhances the current recognition, and the ion concentration polarization across nanopore openings raises the entity capture rate, thereby being capable of improving the performance of electrophoresis-based biosensors. The results gathered provide necessary information for designing nanopore-based biosensor devices.

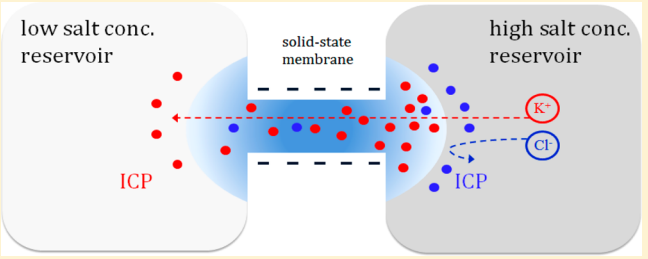


## INTRODUCTION

Recently, salt concentration gradient has drawn much attention for its potential applications in many areas. A charged entity immersed in an electrolyte solution established an ionic cloud richer in counterions surrounding its surface, known as an electrical double layer (EDL).[1] This layer is distorted when a salt concentration gradient is applied, resulting in a diffusiophoretic migration, or diffusiophoresis.[2,3] Both experimental and theoretical attempts have been made on this phenomenon,[4−8] and it has been applied practically.[9−12]

The flow of an electrolyte solution driven by an applied salt concentration gradient near a charged surface, known as capillary osmosis (or diffusioosmosis), is also of much fundamental and practical interest. This phenomenon arises from two mechanisms:[13−15] the tangential salt concentration gradient induces an excess pressure in EDL, and the difference in ionic diffusivities establishes a background electric field, $\mathbf{E}_{\text{diffusivity}}$. The former yields a chemiosmotic flow, and the latter exerts an electric body force on the liquid in EDL, yielding an electroosmotic flow. Diffusioosmosis was analytically studied for the cases of a solid cylindrical pore,[14−16] a planar wall,[13,17,18] and a porous medium.[19] Experimental attempts concerning capillary osmosis were also made.[20] Lin and Prieve,[21] for example, illustrated the existence of a diffusion potential across a porous membrane subject to an applied salt concentration gradient. Available theoretical results, such as an infinitely long cylindrical pore and a very large planar surface, are mainly one-dimensional. Although this simplifies drastically the mathematical analysis, several potentially significant effects are overlooked. In an infinitely long cylindrical pore, for example, the axial electric potential gradient vanishes, and the end effects of both the electric and the flow fields are neglected. These effects can be significant, however, in cases where the length scale of a device comes to submicrometer or even nanometer order. Another assumption usually made in previous analyses is that the applied salt concentration gradient is weak so that a simplified Poisson−Nernst−Planck (PNP) model applies. This simplification neglects the nonlinear effect of the applied salt concentration gradient, which can be interesting and significant.

Recent nanopore-based experiments suggest a novel scenario for biological sensors.[22−25] In these cases, a device usually comprises a solid-state nanopore connecting two relatively large reservoirs. A charged entity in one reservoir migrates as a response to an applied electric field through the nanopore to the other reservoir, and the ionic current blockade is monitored as it passes through. A salt concentration of 1−100 mM yields an EDL thickness that is comparable to the typical pore radius (3−30 nm).[22−26] In a nanopore filled with counterion-rich fluid where EDL overlaps, effects such as ion selectivity[27] and ion concentration polarization (ICP)[28,29] were reported. ICP yields a local electric field adjacent to the nanopore openings, thereby having potential applications.[30−32]

Compared to relevant analyses for the electroosmosis in a charged nanopore, those for the corresponding capillary osmosis (or diffusioosmosis) are still very limited. Qian et al.[33] investigated the diffusioosmosis in a nanoslit. Joo et al.[34]

**Received:** May 21, 2013
**Revised:** July 9, 2013
**Published:** July 17, 2013





dx.doi.org/10.1021/la401925n | Langmuir 2013, 29, 9598−9603

studied the diffusiophoresis of a cylindrical particle in a charged nanopore. Because the axial length scale in these analyses is large, neither ion selectivity nor ICP is important, and therefore, they are neglected. In a nanopore-based experiment, Wanunu et al.[12] demonstrated that applying a salt concentration gradient is capable of enhancing both particle capture efficiency and current signal recognition.

Motivated by rapid advances in nanopore-based sensing technologies, we study the flow of a salt solution in a charged solid-state nanopore connecting two large reservoirs driven by an applied salt concentration gradient. Adopting a continuum-based model composing a set of coupled PNP and Stokes equations, the nanopore geometry and the reservoir salt concentrations are examined for their influences on the behavior of the system under consideration. This is the first theoretical attempt on the analysis of the basic phenomena/mechanisms associated with the capillary osmosis (or diffusioosmosis) flow in a nanopore of finite length.

## ■ ANALYSIS

As shown in Figure 1, we consider a negatively charged cylindrical nanopore of length $l_p$ and radius $b_p$ connecting two large reservoirs filled with aqueous solutions of different salt concentrations, which establishes a concentration gradient across the nanopore. The liquid phase is a Newtonian, incompressible fluid of viscosity $\eta$ containing $z_1$:$z_2$ electrolytes, with $z_1$ and $z_2$ being the valences of cations and anions, respectively, and $\alpha = -z_2/z_1$. The cylindrical coordinates are adopted with the origin at the center of the nanopore. Note that only the $(r,z)$ domain needs be considered in our case.

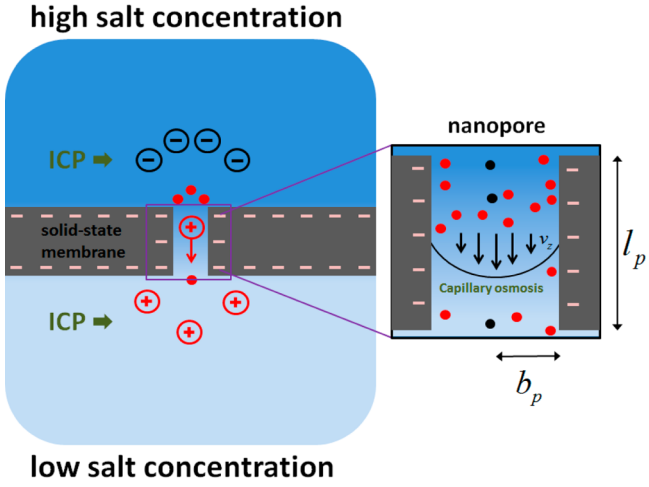


**Figure 1.** Capillary osmosis and ion concentration polarization (ICP) in a negatively charged solid-state nanopore of length $l_p$ and radius $b_p$ connecting two large reservoirs filled with aqueous solutions of different salt concentrations, which establishes a concentration gradient across the nanopore.

A continuum-based model comprising coupled PNP equations and Stokes equations is adopted to describe the present problem. If we let $\psi(r,z)$, $C_j(r,z)$, $\mathbf{v}(r,z)$, and $p(r,z)$ be the electric potential, the molar concentration of ionic species $j$, the fluid velocity, and the pressure, respectively, then[7,35]

$$-\varepsilon\Delta\psi = \rho \tag{1}$$

$$\mathbf{f}_j = C_j\mathbf{v} - D_j\left(\nabla C_j + \frac{z_jF}{k_BT}C_j\nabla\psi\right) \tag{2}$$

$$\nabla\cdot\mathbf{f}_j = 0 \tag{3}$$

$$\nabla\cdot\mathbf{v} = 0 \tag{4}$$

$$-\nabla p + \eta\Delta\mathbf{v} - \rho\nabla\psi = 0 \tag{5}$$

$\nabla$ and $\Delta$ are the gradient operator and the Laplace operator, respectively. $\varepsilon$, $F$, $k_B$, and $T$ are the permittivity, Faraday constant, Boltzmann constant, and the absolute temperature, respectively. $\rho = \sum z_jFC_j$ is the spatial charge density. $\mathbf{f}_j$ and $D_j$ are the flux and the diffusivity of ion species $j$, respectively. $\mathbf{v} = v_r\mathbf{e}_r + v_z\mathbf{e}_z$ with $v_r$ ($v_z$) and $\mathbf{e}_r$ ($\mathbf{e}_z$) being the $r$ ($z$) component of $\mathbf{v}$ and the unit vector in the $r$ ($z$) direction, respectively. The continuum-based model, eqs 1−5, is capable of capturing the physics of the nanopore if its radius exceeds 3 nm.[36−38]

The boundary conditions associated with eqs 1−5 are based on the following assumptions: (i) The ionic concentration at the ends of the low (high) salt concentration reservoir is maintained at the bulk value $C_1 = \alpha C_2 = C_{low}$ ($C_1 = \alpha C_2 = C_{high}$). (ii) No external electric field is applied, and therefore, the electric potential differences at the ends of both reservoirs come only from $\mathbf{E}_{diffusivity}$, the electric field arising from the difference in ionic diffusivities. $\psi = \phi$ ($\psi = 0$) in the high (low) concentration reservoir, where $\phi$ needs be determined as when the ionic current vanishes in both reservoirs.[32] (iii) The solid-state membrane is ion-impenetrable, $\mathbf{n}\cdot\mathbf{f}_j = 0$, with $\mathbf{n}$ being the unit normal vector directed into the liquid phase. It is nonslip ($\mathbf{v} = 0$) and has the surface charge density $\sigma_b$ ($-\mathbf{n}\cdot\varepsilon\nabla\psi = \sigma_b$). (iv) No external pressure is applied.

If we denote $C_{avg} = (C_{high} + C_{low})/2$ and $\Lambda = C_{high}/C_{low}$ as the averaged salt concentration and the imposed salt concentration ratio, respectively, then[34]

$$C_{high} = \frac{2\Lambda C_{avg}}{1+\Lambda} \tag{6}$$

$$C_{low} = \frac{2C_{avg}}{1+\Lambda} \tag{6a}$$

The boundary conditions are summarized in Supporting Information.

The present problem is solved numerically by COMSOL MultiPhysics (version 4.3a, www.comsol.com) operated in a high-performance cluster. Equations 1−5 are solved for $\psi(r,z)$, $C_j(r,z)$, $\mathbf{v}(r,z)$, and $p(r,z)$ subject to the boundary conditions specified in eqs S1−S13 of Supporting Information. The applicability of the software adopted is verified by solving the limiting cases of electroosmosis where analytical solutions are available[39] and other numerical treatment.[7,35,40,41] Details about the verification are presented in the Supporting Information.

Deryaguin et al.[42] derived an analytical expression for the diffusiophoretic velocity of an isolated particle, which is the asymptotic result of our model when the nanopore is infinitely long and the associated double layer is thin. This asymptotic behavior is verified in Supporting Information.

## ■ RESULTS AND DISCUSSION

For illustration, we assume that the background electrolyte is KCl, and an extra KCl concentration gradient is imposed.[12] Because $D_{K^+} \cong D_{Cl^-} \cong 2 \times 10^{-9}$ m$^2$/s, $\mathbf{E}_{diffusivity} \cong 0$ ($\phi \cong 0$), only chemiosmosis needs be considered. Assume that the


dx.doi.org/10.1021/la401925n | Langmuir 2013, 29, 9598−9603

radius and the length of both reservoirs are 150 and 250 nm, respectively. Other parameters used are $\varepsilon = 7.08 \times 10^{-10}$ F/m, $F = 96\,485$ C/mol, $T = 298$ K, $\eta = 10^{-3}$ Pa·s, and $\sigma_b = -20 \times 10^{-3}$ C/m$^2$.

**Induced Electric Field and Capillary Osmosis.** As illustrated in Figure 1, when a salt concentration gradient is applied across the nanopore, the liquid is driven diffusively from the high salt concentration reservoir toward the low salt concentration reservoir. Because the concentration of counterions (cations) in the EDL on the high salt concentration side is higher than that on the low salt concentration side, a local electric field that points toward the low concentration salt side is induced. This local electric field, which is attributed to double layer polarization (DLP), is defined as $\mathbf{E}_{DLP}$.[7,35]

Figure 2 shows the variation in the strength of the axial local electric field coming from $\mathbf{E}_{DLP}$, $E = \mathbf{e}_z \cdot (-\nabla\psi)$, with $r$ at $z = 0$.

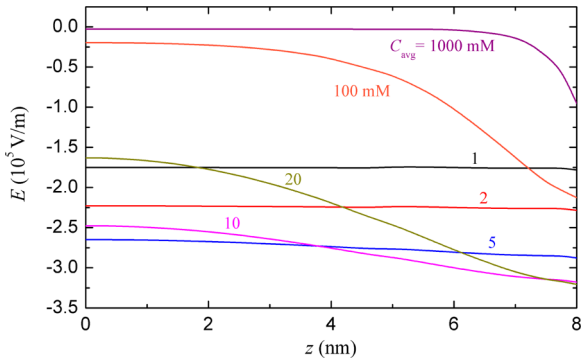


**Figure 2.** Variations of the strength of axial local electric field $E$ with the radial distance $r$ at $z = 0$ for various levels of $C_{avg}$ at $\Lambda = 5$, $b_p = 8$ nm, and $l_p = 80$ nm.

As can be seen, $E$ is nearly constant for $C_{avg} \leq 5$ mM, implying significant EDL overlapping. As the salt concentration increases, so does the ionic strength and, therefore, the strength of $\mathbf{E}_{DLP}$. If $C_{avg} \geq 10$ mM, EDL overlaps only partially, and $E$ decreases with increasing $C_{avg}$. This is because an increase in $C_{avg}$ reduces not only the EDL thickness but also the surface potential of the nanopore. Note that at $C_{avg} = 1000$ mM, $E$ almost vanishes at the center of the nanopore, implying that EDL no longer overlaps. Figure 2 also suggests that $|E|$ has a local maximum as $C_{avg}$ varies.

Because the liquid in a negatively charged nanopore contains excess cations (counterions), $\mathbf{E}_{DLP}$ exerts an electric body force on the liquid, yielding a capillary osmotic (or chemiosmotic) flow toward the low salt concentration side. Figure 3 shows the variation of the axial liquid velocity $v_z$ with the radial distance $r$ at the nanopore center ($z = 0$) for the case of Figure 2. As can be seen in Figure 3, $v_z$ is negative, which is expected, and $|v_z|$ decreases monotonically with increasing $r$. Intuitively, if an extra salt concentration gradient is applied to enhance the particle mobility in an electrophoresis-based biosensing device,[12] a faster capillary osmotic flow is capable of raising current recognition. In the case where a particle migrates from the low salt concentration reservoir to the high salt concentration reservoir driven by an applied electric field, its mobility will be reduced by that osmotic flow. Similar to the behavior of $E$ in Figure 2, $|v_z|$ in Figure 3 also has a maximum as $C_{avg}$ varies.

**Influences of Averaged Salt Concentration and Nanopore Size.** In the case where an electric field is applied (i.e., electrophoresis), Ai and Qian[43] found that particles tend

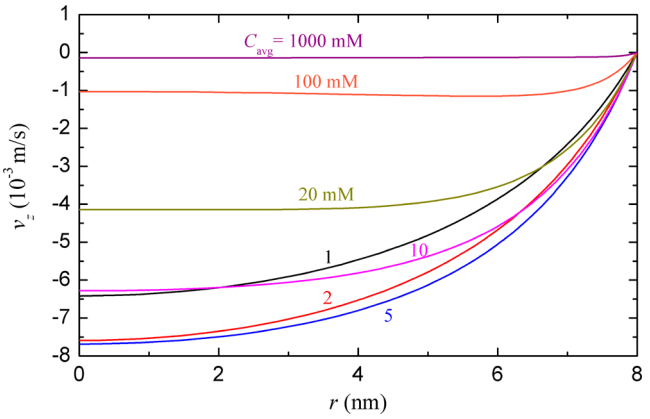


**Figure 3.** Variations of the axial liquid velocity $v_z$ with the radial distance $r$ at $z = 0$ for the case of Figure 2.

to align on the $z$ axis ($r = 0$) as they approach the nanopore opening. Therefore, the capillary osmosis velocity at $r = 0$, $v_{z,0}$, is chosen to characterize the capillary osmotic flow inside the nanopore. Figure 4 reveals that $|v_{z,0}|$ has a local maximum as

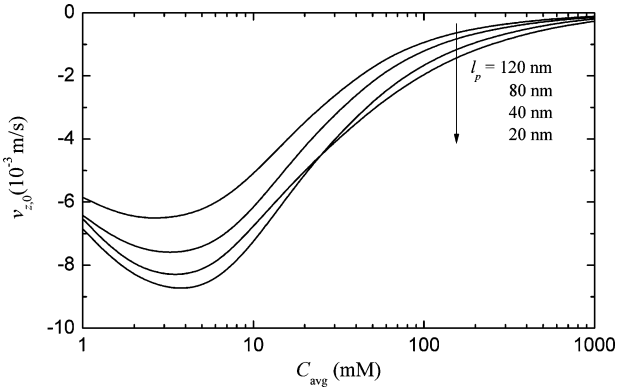


**Figure 4.** Variations of the axial fluid velocity $v_{z,0}$ with the averaged salt concentration $C_{avg}$ at $z = 0$ for various values of $l_p$ at $\Lambda = 5$ and $b_p = 8$ nm.

$C_{avg}$ varies, and the shorter the nanopore (smaller $l_p$), the higher the $C_{avg}$ at which the local maximum of $|v_{z,0}|$ occurs. In addition, the shorter the nanopore, the larger the $|v_{z,0}|$. Note that the salt concentration gradients near the nanopore openings are much stronger than that at a point far from the nanopore. As a result, although the imposed salt concentrations remain the same ($\Lambda = C_{high}/C_{low} = 5$), the effective salt concentration gradient across the nanopore varies with its length. The shorter the nanopore, the stronger the concentration gradient and, therefore, the stronger the induced electric field $\mathbf{E}_{DLP}$ and the faster the capillary osmotic flow. However, if $l_p$ is too short (ca. 40 nm) and $C_{avg}$ is low (thick double layer), $|v_{z,0}|$ might decrease with decreasing $l_p$. This is because under these conditions the nanopore surface potential decreases due to a lack of sufficiently large charged boundary. Therefore, if capillary osmosis is adopted to enhance the current recognition in an electrophoresis-based nanodevice, the nanopore length (membrane thickness) should not be shorter than ca. 40 nm.

Figure 5 illustrates the influence of $C_{avg}$ on $v_{z,0}$ at various values of the nanopore radius $b_p$. This figure reveals that $|v_{z,0}|$ has a local maximum as $C_{avg}$ varies, and the level of $C_{avg}$ at which the local maximum of $|v_{z,0}|$ varies with $b_p$. This implies


dx.doi.org/10.1021/la401925n | Langmuir 2013, 29, 9598−9603

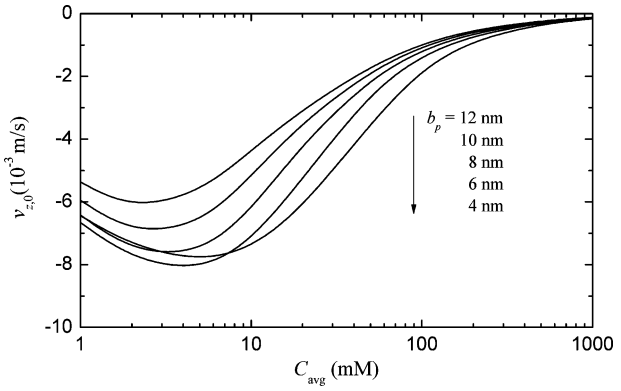


**Figure 5.** Variations of the axial fluid velocity $v_{z,0}$ with the averaged salt concentration $C_{avg}$ at $z = 0$ for various values of $b_p$ at $\Lambda = 5$ and $l_p = 80$ nm.

that for a nanopore of larger $b_p$, a more dilute $C_{avg}$ is needed for EDL overlapping to be significant, which is expected. Figure 5 also suggests that if $C_{avg}$ is sufficiently high (>10 mM), the smaller the $b_p$, the larger the $|v_{z,0}|$. Note that for a fixed $C_{avg}$, a smaller $b_p$ results in not only a more significant EDL overlapping but also a higher nanopore surface potential. However, if $C_{avg}$ is too low, $|v_{z,0}|$ decreases with decreasing $b_p$ due to the wall effect. We conclude that if capillary osmosis is adopted to enhance the current recognition in an electrophoresis-based nanodevice, $C_{avg}$, $l_p$, and $b_p$ should range within 1−10 mM, 30−50 nm, and 5−8 nm, respectively.

**Ion Concentration Polarization (ICP).** In this section we present, for the first time, the ICP occurring near the openings of a nanopore induced by an applied salt concentration gradient. Figure 6 illustrates the variation of the electric

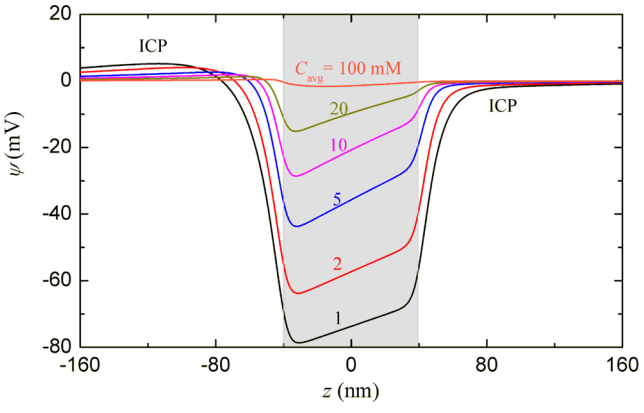


**Figure 6.** Variations of the electric potential $\psi$ long the $z$ axis ($r = 0$) for various levels of $C_{avg}$ at $\Lambda = 5$, $b_p = 8$ nm, and $l_p = 80$ nm; the gray region ($|z| < 40$ nm) denotes the nanopore interior.

potential $\psi$ along the $z$ axis. Here, $\psi$ is negative inside the nanopore ($-40$ nm $< z <$ 40 nm) because it is negatively charged. In addition, the slope of $\psi$ is positive in that region, which is consistent with the results shown in Figure 2, where $\mathbf{E}_{DLP}$ directs to the low salt concentration reservoir.

It is interesting to observe in Figure 6 that $\psi$ is slightly positive (negative) near the low (high) salt concentration side opening of the nanopore. As is schematically represented in Figure 7, this explains both ion selectivity and ICP. Intuitively, the applied salt concentration gradient drives diffusively both cations and anions toward the low concentration reservoir.

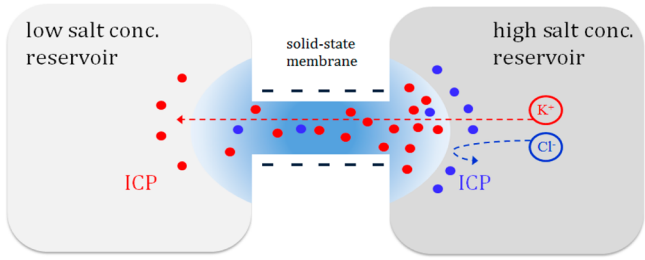


**Figure 7.** Mechanism of ICP; the light blue region denotes the EDL established by nanopores.

However, the negatively charged nanopore attracts cations (counterions) and repels anions (co-ions), making it easier for cations to diffuse through the nanopore. As a result, cations (anions) accumulate on the low (high) concentration side opening of the nanopore, as illustrated in Figure 8, thereby inducing a local positive electric potential on the low concentration side opening of the nanopore, as shown in Figure 6.

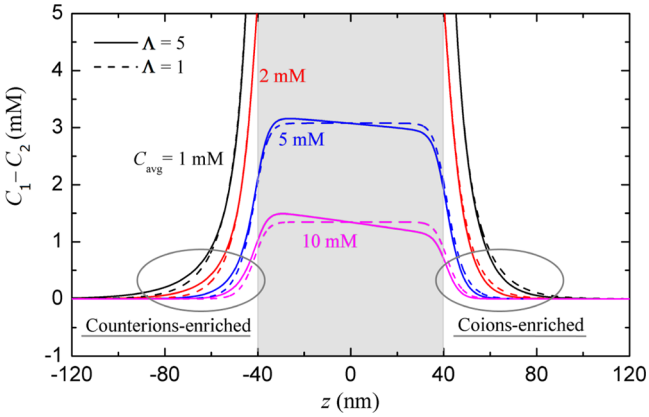


**Figure 8.** Variations in the ion concentration difference ($C_1 - C_2$) along the $z$ axis ($r = 0$) for two levels of $\Lambda$ at $b_p = 8$ nm and $l_p = 80$ nm; the gray region ($|z| <40$ nm) denotes the nanopore interior.

Applying an extra salt concentration gradient across a nanopore device, Wanunu et al.[12] experimentally demonstrated that the capture rate of an electrophoresis-based sensor can be enhanced. This can be explained by the unlabeled particle in their study, which is usually negatively charged, being attracted electrically toward the nanopore opening by the previously mentioned positive electric potential on the low concentration side opening of the nanopore (i.e., ICP). Our results also reveal that, in general, the shorter the nanopore and/or the smaller its radius, the stronger the capillary osmotic flow. In electrophoretic navigating applications, analyzing the influence of nanopore geometry on the forces (electric and hydrodynamic) acting on unlabeled particles and that on their mobility is necessary. Assessing the significance of an applied salt concentration field relative to that of an applied electric field also deserves further detailed study.

## ■ CONCLUSIONS

Adopting a continuum-based model, we analyzed theoretically the capillary osmotic flow in a negatively charged solid-state nanopore connecting two large reservoirs subject to an applied salt concentration gradient and the ion concentration polar-


dx.doi.org/10.1021/la401925n | Langmuir 2013, 29, 9598−9603

ization across the nanopore. We show that the capillary osmotic flow is from the high salt concentration reservoir to the low salt concentration reservoir, and the flow velocity has a maximum as the bulk salt concentrations of the reservoirs vary. In general, the shorter the nanopore and/or the smaller its radius, the faster the osmotic flow is. If capillary osmosis is adopted to enhance the current recognition in an electrophoresis-based nanodevice, the average salt concentration of two reservoirs, the nanopore length, and its radius should range within 1−10 mM, 30−50 nm, and 5−8 nm, respectively. The present analysis demonstrates the ion selectivity of a nanopore observed experimentally and the ICP across its two ends. The results gathered provide necessary theoretical background for further design of diffusioosmosis relevant nanodevices.

## ■ ASSOCIATED CONTENT

### Supporting Information

Additional material as noted in the text. This material is available free of charge via the Internet at http://pubs.acs.org.

## ■ AUTHOR INFORMATION


### Corresponding Author

*J.-P.H.: tel, 886-2-23637448; fax, 886-2-23623040; e-mail, jphsu@ntu.edu.tw. S.T.: e-mail, topology@mail.tku.edu.tw


### Notes

The authors declare no competing financial interest.

## ■ ACKNOWLEDGMENTS

This work is supported by the National Science Council of the Republic of China.

## ■ REFERENCES


(1) Hunter, R. J. *Foundations of Colloid Science*; Oxford University: Oxford, 1989; Vol. *1*.

(2) Dukhin, S. S.; Deryaguin, B. V. *Surface and Colloid Science*; Wiley: New York, 1974; Vol. *7*.

(3) Brady, J. F. Particle motion driven by solute gradients with application to autonomous motion: Continuum and colloidal perspectives. *J. Fluid Mech.* **2011**, *667*, 216−259.

(4) Lechnick, W. J.; Shaeiwitz, J. A. Measurement of diffusiophoresis in liquids. *J. Colloid Interface Sci.* **1984**, *102*, 71−87.

(5) Ebel, J. P.; Anderson, J. L.; Prieve, D. C. Diffusiophoresis of latex particles in electrolyte gradients. *Langmuir* **1988**, *4*, 396−406.

(6) Lou, J.; Shih, C. Y.; Lee, E. Diffusiophoresis of concentrated suspensions of spherical particles with charge-regulated surface: Polarization effect with nonlinear Poisson−Boltzmann equation. *Langmuir* **2010**, *26*, 47−55.

(7) Liu, K. L.; Hsu, J. P.; Hsu, W. L.; Yeh, L. H.; Tseng, S. Diffusiophoresis of a polyelectrolyte in a salt concentration gradient. *Electrophoresis* **2012**, *33*, 1068−1078.

(8) Huang, P. Y.; Keh, H. J. Diffusiophoresis of a spherical soft particle in electrolyte gradients. *J. Phys. Chem. B* **2012**, *116*, 7575−7589.

(9) Pérez, J. S.; Fery, D. D. Behavior of the inadvertent pH transient formed by a salt gradient in the ion-exchange chromatography of proteins. *Biotechnol. Prog.* **2005**, *21*, 902−910.

(10) Abécassis, B.; Cottin-Bizonne, C.; Tbert, C.; Ajdari, A.; Bocquet, L. Boosting migration of large particles by solute contrasts. *Nat. Mater.* **2008**, *7*, 785−789.

(11) Palacci, J.; Abécassis, B.; Cottin-Bizonne, C.; Tbert, C.; Bocquet, L. Colloidal motility and pattern formation under rectified diffusiophoresis. *Phys. Rev. Lett.* **2010**, *104*, 138302.

(12) Wanunu, M.; Morrison, W.; Rabin, Y.; Grosberg, A. Y.; Meller, A. Electrostatic focusing of unlabelled DNA into nanoscale pores using a salt gradient. *Nat. Nanotechnol.* **2010**, *5*, 160−165.

(13) Prieve, D. C.; Anderson, J. L.; Ebel, J. P.; Lowell, M. E. Motion of a particle generated by chemical gradient. 2. Electrolytes. *J. Fluid Mech.* **1984**, *148*, 247−269.

(14) Ma, H. C.; Keh, H. J. Diffusioosmosis of electrolyte solutions in a fine capillary slit. *J. Colloid Interface Sci.* **2006**, *298*, 476−486.

(15) Keh, H. J.; Ma, H. C. Diffusioosmosis of electrolyte solutions in a fine capillary tube. *Langmuir* **2007**, *23*, 2879−2886.

(16) Fair, J. C.; Osterle, J. F. Reverse electrodialysis in charged capillary membranes. *J. Chem. Phys.* **1971**, *54*, 3307−3316.

(17) Anderson, J. L. Colloid transport by interfacial forces. *Annu. Rev. Fluid Mech.* **1989**, *21*, 61−99.

(18) Keh, H. J.; Ma, H. C. Diffusioosmosis of electrolyte solutions along a charged plane wall. *Langmuir* **2005**, *21*, 5461−5467.

(19) Keh, H. J.; Hsu, L. Y. Diffusioosmotic flow of electrolyte solutions in fibrous porous media at arbitrary zeta potential and double-layer thickness. *MicrofluidNanofluid* **2009**, *7*, 773−781.

(20) Dukhin, S. S. Non-equilibrium electric surface phenomena. *Adv. Colloid Interface Sci.* **1993**, *44*, 1−134.

(21) Lin, M. M. J.; Prieve, D. C. Electromigration of latex induced by a salt gradient. *J. Colloid Interface Sci.* **1983**, *95*, 327−339.

(22) Singer, A.; Wanunu, M.; Morrison, W.; Kuhn, H.; Kamenetskii, M. K.; Meller, A. Nanopore based sequence specific detection of duplex DNA for genomic profiling. *Nano Lett.* **2010**, *10*, 738−742.

(23) Keyser, U. F. Controlling molecular transport through nanopores. *J. R. Soc. Interface* **2011**, *8*, 1369−1378.

(24) Bahrami, A.; Doğan, F.; Japrung, D.; Albrecht, T. Solid-state nanopores for biosensing with submolecular resolution. *Biochem. Soc. Trans.* **2012**, *40*, 624−628.

(25) Scheicher, R. H.; Grigoriev, A. DNA sequencing with nanopores from an ab initio perspective. *J. Mater. Sci.* **2012**, *47*, 7439−7446.

(26) Yeh, L. H.; Zhang, M.; Qian, S.; Hsu, J. P.; Tseng, S. Ion concentration polarization in polyelectrolyte-modified nanopores. *J. Phys. Chem. C* **2012**, *116*, 8672−8677.

(27) Daiguji, H. Ion transport in nanofluidic channels. *Chem. Soc. Rev.* **2010**, *39*, 901−911.

(28) Schoch, R. B.; Han, J. Y.; Renaud, P. Transport phenomena in nanofluidics. *Rev. Mod. Phys.* **2008**, *80*, 839−883.

(29) Zangle, T. A.; Mani, A.; Santiago, J. G. Theory and experiments of concentration polarization and ion focusing at microchannel interfaces. *Chem. Soc. Rev.* **2010**, *39*, 1014−1035.

(30) Hlushkou, D.; Perry, J. M.; Jacobson, S. C.; Tallarek, U. Propagating concentration polarization and ionic current rectification in a nanochannel device. *Anal. Chem.* **2012**, *84*, 267−274.

(31) Huang, K. D.; Yang, R. J. A nanochannel-based concentrator utilizing the concentration polarization. *Electrophoresis* **2008**, *29*, 4862−4870.

(32) Kwak, R.; Kim, S. J.; Han, J. Continuous-flow biomolecule and cell concentrator by ion concentration polarization. *Anal. Chem.* **2011**, *83*, 7348−7355.

(33) Qian, S.; Das, B.; Luo, X. Diffusioosmotic flows in slit nanochannels. *J. Colloid Interface Sci.* **2007**, *315*, 721−730.

(34) Joo, S. W.; Lee, S. Y.; Liu, J.; Qian, S. Diffusiophoresis of an elongated cylindrical nanopore along the axis of a nanopore. *Chem. Phys. Chem.* **2010**, *11*, 3281−3290.

(35) Hsu, J. P.; Liu, K. L.; Hsu, W. L.; Yeh, L. H.; Tseng, S. Diffusiophoresis of a charge-regulated spherical particle normal to two parallel disks. *J. Phys. Chem. B* **2010**, *114*, 2766−2778.

(36) van Dorp, S.; Keyser, U. F.; Dekker, N. H.; Dekker, C.; Lemay, S. G. Origin of the electrophoretic force on DNA in solid-state nanopores. *Nat. Phys.* **2009**, *5*, 347−351.

(37) He, Y. H.; Tsutsui, M.; Fan, C.; Taniguchi, M.; Kawai, T. Controlling DNA translocation through gate modulation of nanopore wall surface charges. *ACS Nano* **2011**, *5*, 5509−5518.

(38) Yeh, L. H.; Zhang, M. K.; Qian, S.; Hsu, J. P. Regulating DNA translocation through functionalized soft nanopores. *Nanoscale* **2012**, *4*, 2685−2693.

(39) Rice, C. L.; Whitehead, R. Electrokinetic flow in a narrow cylindrical capillary. *J. Phys. Chem.* **1965**, *69*, 4017−4024.

(40) Yeh, L. H.; Hsu, J. P. Effects of double-layer polarization and counterion condensation on the electrophoresis of polyelectrolytes. *Soft Matter* **2011**, *7*, 396−411.
(41) Liu, K. L.; Hsu, J. P.; Tseng, S. Diffusiophoresis of a polyelectrolyte in a salt concentration gradient. *Electrophoresis* **2012**, *32*, 3053−3061.
(42) Deryaguin, B. V.; Ul'berg, Z. R.; Dukhin, S. S. Microscopic investigation of diffusiophoresis in aqueous and nonaqueous solutions. *Colloid J. USSR* **1986**, *48*, 570−573.
(43) Ai, Y.; Qian, S. Z. Electrokinetic particle translocation through a nanopore. *Phys. Chem. Phys.* **2011**, *13*, 4060−4071.